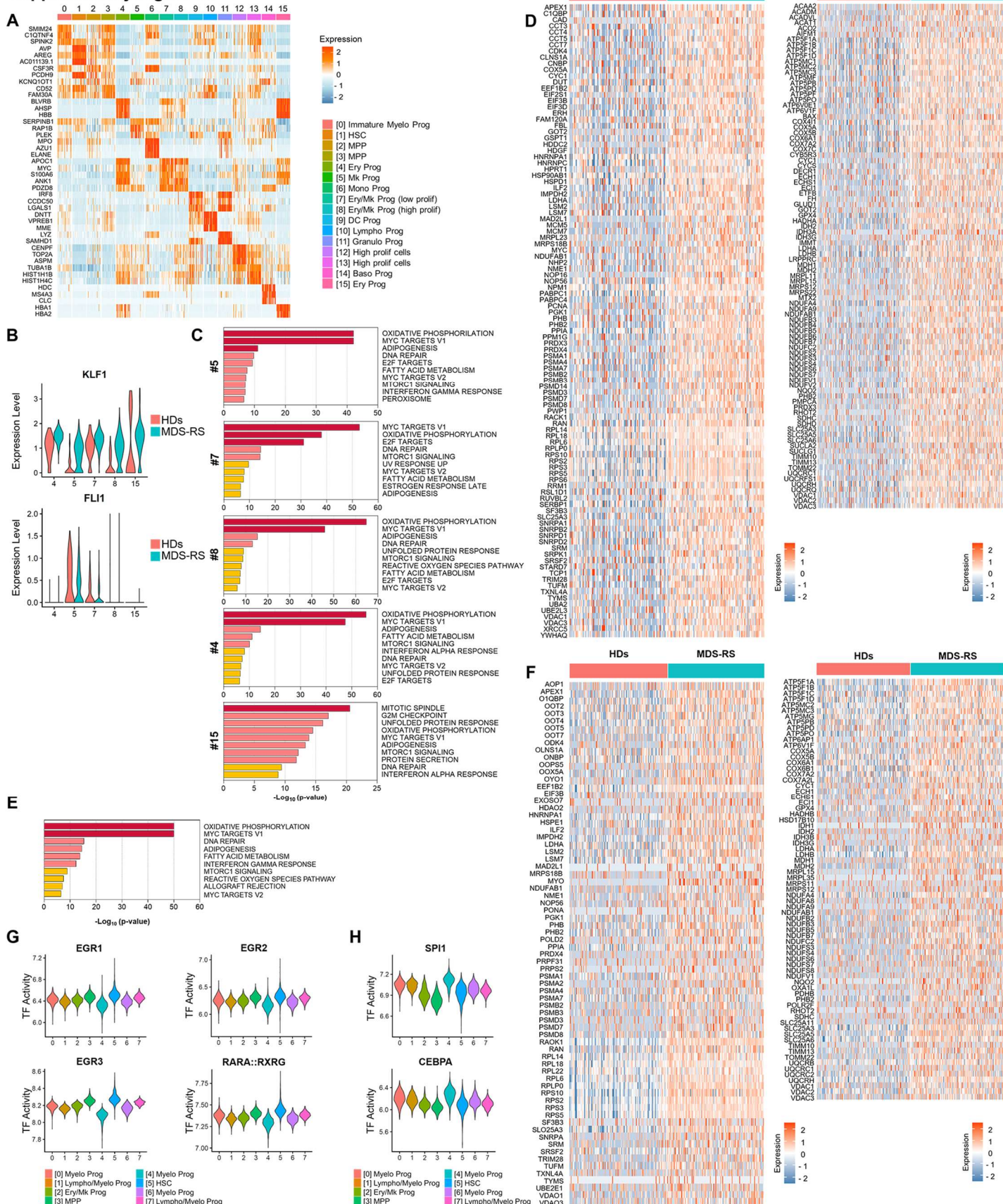


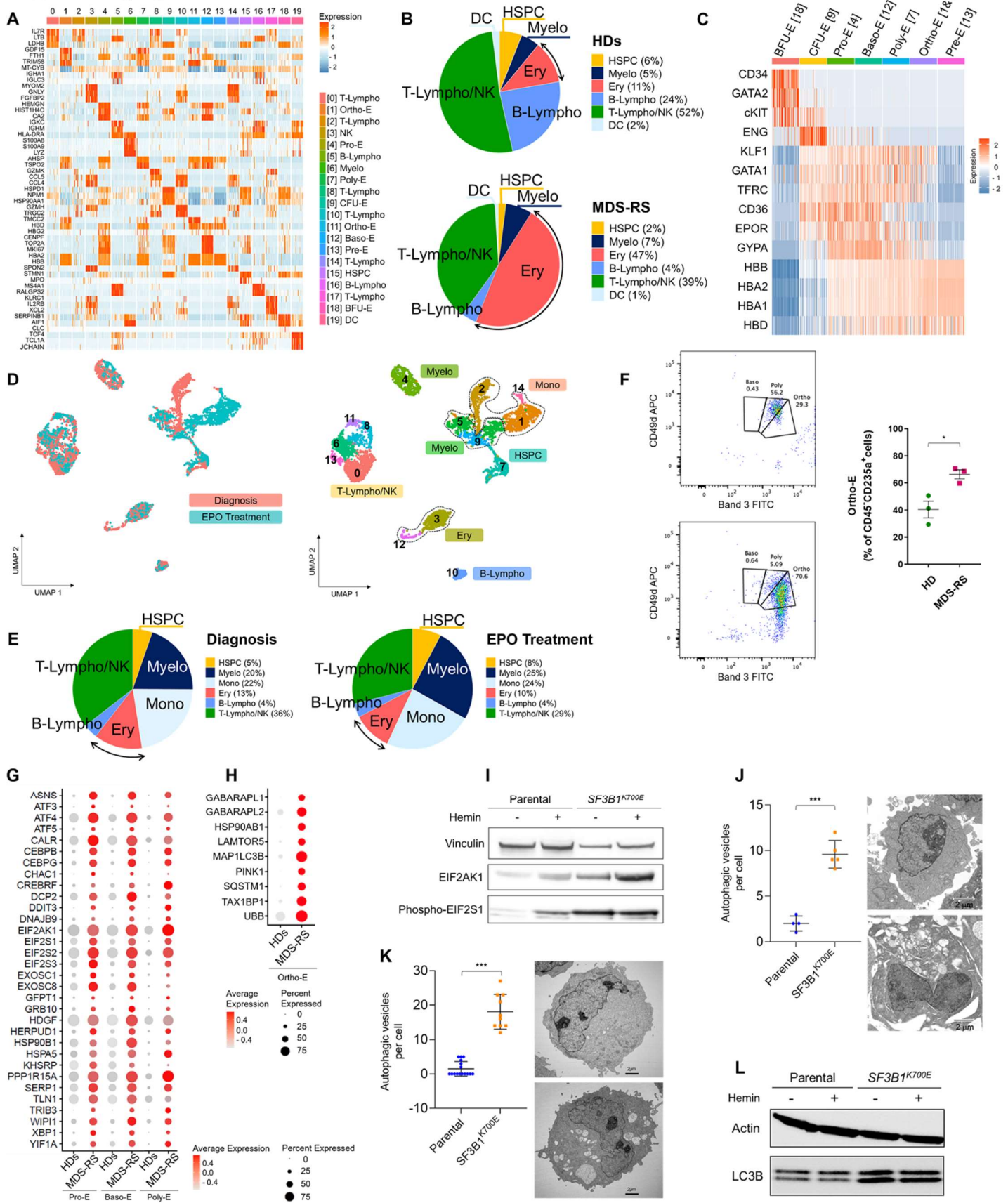
Supplementary Figure S1



Supplementary Figure S1. SF3B1^{MT} do not affect erythropoiesis at the level of HSPCs

(A) Heatmap of the expression of the top 3 genes enriched in each of the 16 clusters shown in Figure 1A. **(B)** Violin plots of *KLF1* (top) and *FLI1* (bottom) expression across the HD and MDS-RS Ery/Mk clusters shown in Figure 1A. **(C)** Pathway enrichment analysis of the genes that were significantly upregulated in MDS-RS Ery/Mk clusters 5, 7, 8, 4, and 15 as compared with the HD clusters shown in Figure 1A (adjusted $P \leq 0.05$). The top 10 Hallmark gene sets are shown. **(D)** Heatmaps of the expression of the MYC signaling (left) and oxidative phosphorylation (right) pathway genes that were significantly upregulated in the MDS-RS erythroid/megakaryocytic cell clusters as compared with the HD erythroid/megakaryocytic cell cluster shown in Figure 1A. **(E)** Pathway enrichment analysis of the genes that were significantly upregulated in the MDS-RS HSC cluster as compared with the HD HSC cluster shown in Figure 1A (adjusted $P \leq 0.05$). The top 10 Hallmark gene sets are shown. **(F)** Heatmaps of the expression of MYC signaling (left) and oxidative phosphorylation (right) pathway genes that were significantly upregulated in the MDS-RS HSC cluster as compared with the HD HSC cluster shown in Figure 1A. **(G)** Violin plots showing the activities of the TFs EGR1, EGR2, EGR3, and RARA:RXRG across the 8 clusters shown in Figure 1D. **(H)** Violin plots showing the activities of the TFs SPI1 and CEBPA across the 8 clusters shown in Figure 1D.

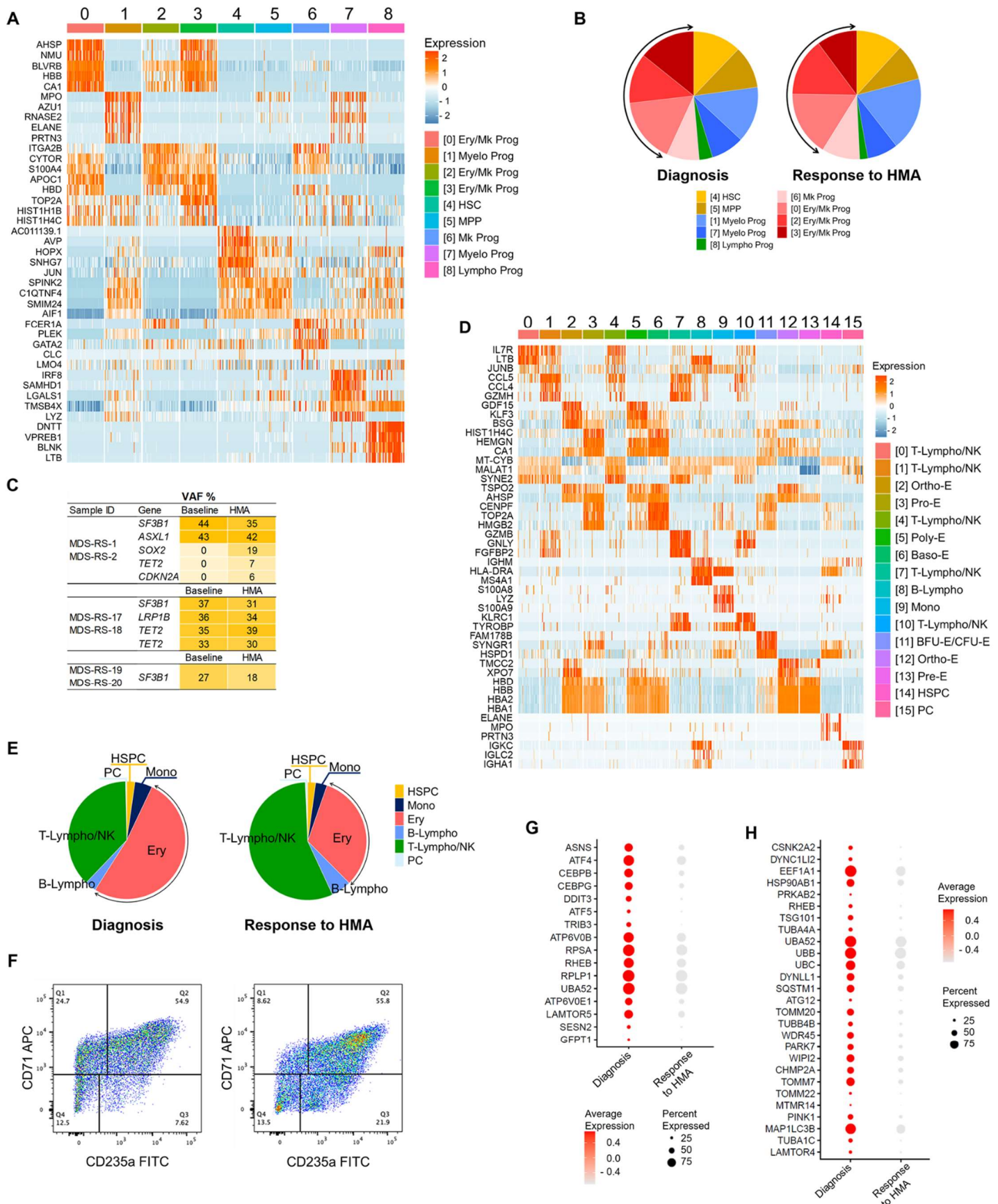
Supplementary Figure S2



Supplementary Figure S2. *SF3B1*^{MT} arrest erythroid terminal differentiation and activate the EIF2AK1-induced response pathway to heme deficiency

(A) Heatmap of the expression of the top 3 genes enriched in each of the 20 clusters shown in Figure 2A. **(B)** Distribution of HD (top) and MDS-RS (bottom) MNCs among the cluster groups shown in Figure 2A defined by distinct lineage differentiation trajectories. HSPC, hematopoietic stem and progenitor cells; Myelo, myeloid cells; Ery, erythroblasts; B-Lympho, B-lymphocytes; T-Lympho/NK, T-lymphocytes and natural killer cells; DC, dendritic cells. Arrows indicate the erythroblastic population. **(C)** Heatmap of the expression of representative surface markers (*CD34*, *cKIT*, *ENG*, *TFRC*, *CD36*, *EPOR*, and *GYPA*), transcriptional factors (*GATA1*, *GATA2*, and *KLF1*), and hemoglobin subunits (*HBB*, *HBA2*, *HBA1*, and *HBD*) across different stages of erythroid differentiation. BFU-E, phenotypic burst forming unit-erythroid cells; CFU-E, phenotypic colony formation unit-erythroid cells; Pro-E, pro-erythroblasts; Baso-E, basophilic erythroblasts; Poly-E, polychromatophilic erythroblasts; Ortho-E, orthochromatic erythroblasts; Pre-E, pre-erythrocytes. **(D)** UMAP plots of scRNA-seq data for single BM MNCs isolated from one patient with *SF3B1*-mutant MDS-RS at the time of diagnosis (n=2,608) and after EPO treatment (n=3,182). Each dot represents one cell. Different colors represent the sample origin (left) and cluster identity (right). HSPC, hematopoietic stem and progenitor cells; Myelo, myeloid cells; Mono, monocytes; Ery, erythroblasts; B-Lympho, B-lymphocytes; T-Lympho/NK, T-lymphocytes and natural killer cells. **(E)** Distribution of MNCs across the clusters shown in Figure S2D. **(F)** Left, representative flow cytometry plots showing the expression of integrin α4 (CD49d) and band 3 in CD45⁺CD235a⁺ erythroblasts from one HD BM sample (top) and one *SF3B1*-mutant MDS-RS BM sample (bottom). Right, frequencies of orthochromatic erythroblasts (Ortho-E) in CD45⁺CD235a⁺ erythroblasts isolated from HD BM samples (n=3) and *SF3B1*-mutant MDS-RS BM samples (n=3). Statistically significant differences were detected using a 2-tailed Student *t*-test. Baso-E, basophilic erythroblasts; Poly-E, polychromatophilic erythroblasts. **(G)** Dot plot of the expression of the genes belonging to the EIF2AK1-mediated pathway that were significantly upregulated in the MDS-RS Pro-E, Baso-E, and Poly-E clusters as compared with the HD Pro-E, Baso-E, and Poly-E clusters shown in Figure 2B. **(H)** Dot plot of the expression of the autophagy pathway genes that were significantly upregulated in the MDS-RS Ortho-E cluster as compared with the HD Ortho-E cluster shown in Figure 2B. **(I)** Representative Western blot analysis of EIF2AK1 and phospho-EIF2S1 in parental and *SF3B1*^{K700E} K562 cells treated with vehicle (-) or hemin (+) for 3 days. Vinculin was used as a loading control. **(J)** Left, number of autophagic vesicles per cell in 4 parental and 4 *SF3B1*^{K700E} K562 cells. Statistically significant differences were detected using a 2-tailed Student *t*-test. Right, representative transmission electron microscopy images of one representative parental cell (top) and one *SF3B1*^{K700E} K562 cell (bottom). Scale bars represent 2 μm. **(K)** Left, number of autophagic vesicles per cell in 16 parental and 10 *SF3B1*^{K700E} K562 cells after 3 days of hemin-induced differentiation. Significant differences were detected using a 2-tailed Student *t*-test. Right, representative transmission electron microscopy images of one representative parental cell (top) and one *SF3B1*^{K700E} K562 cell (bottom). Scale bars represent 2 μm. **(L)** Representative Western blot analysis of LC3B in parental and *SF3B1*^{K700E} K562 cells treated with vehicle (-) or hemin (+) for 3 days. Actin was used as a loading control.

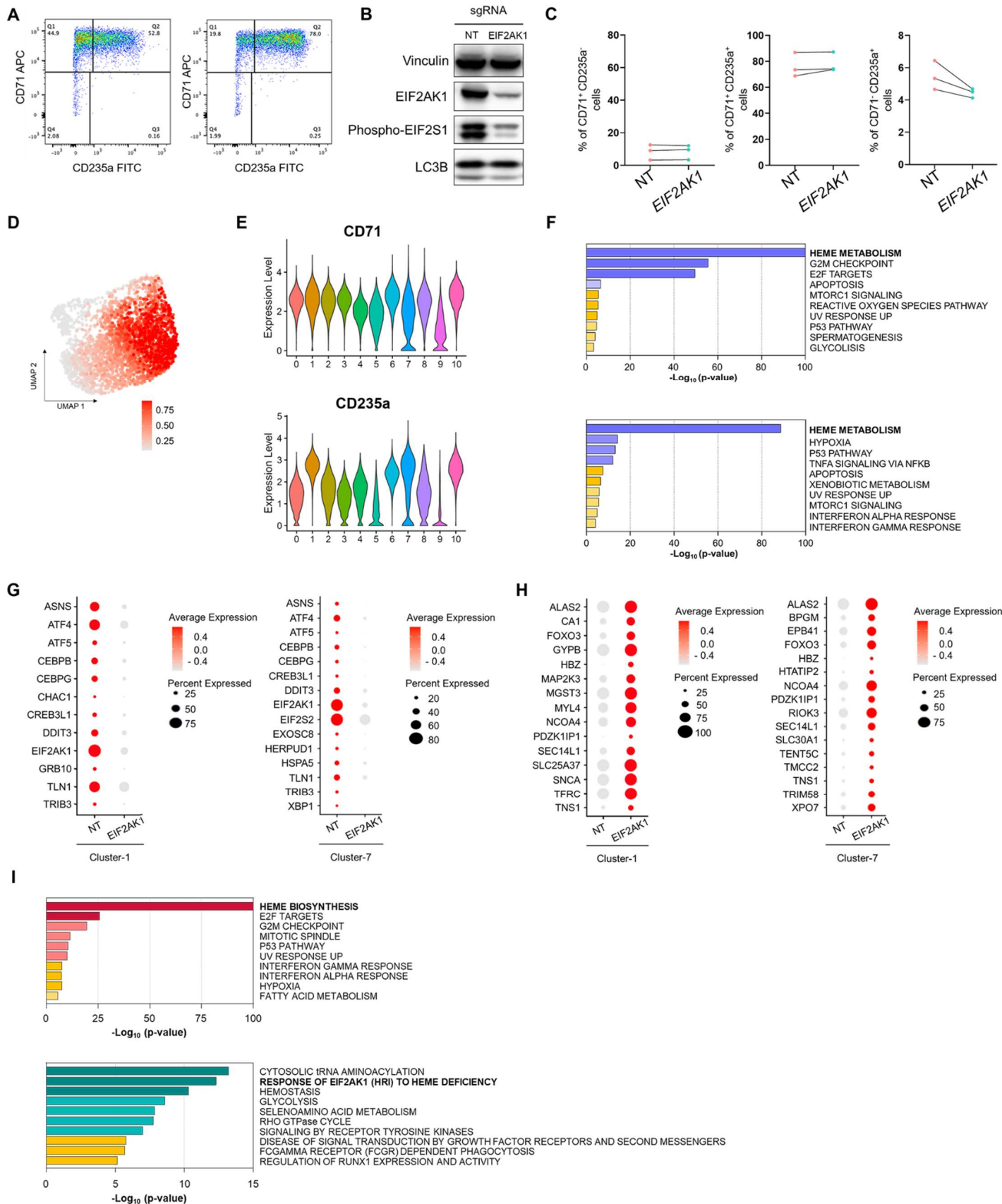
Supplementary Figure S3



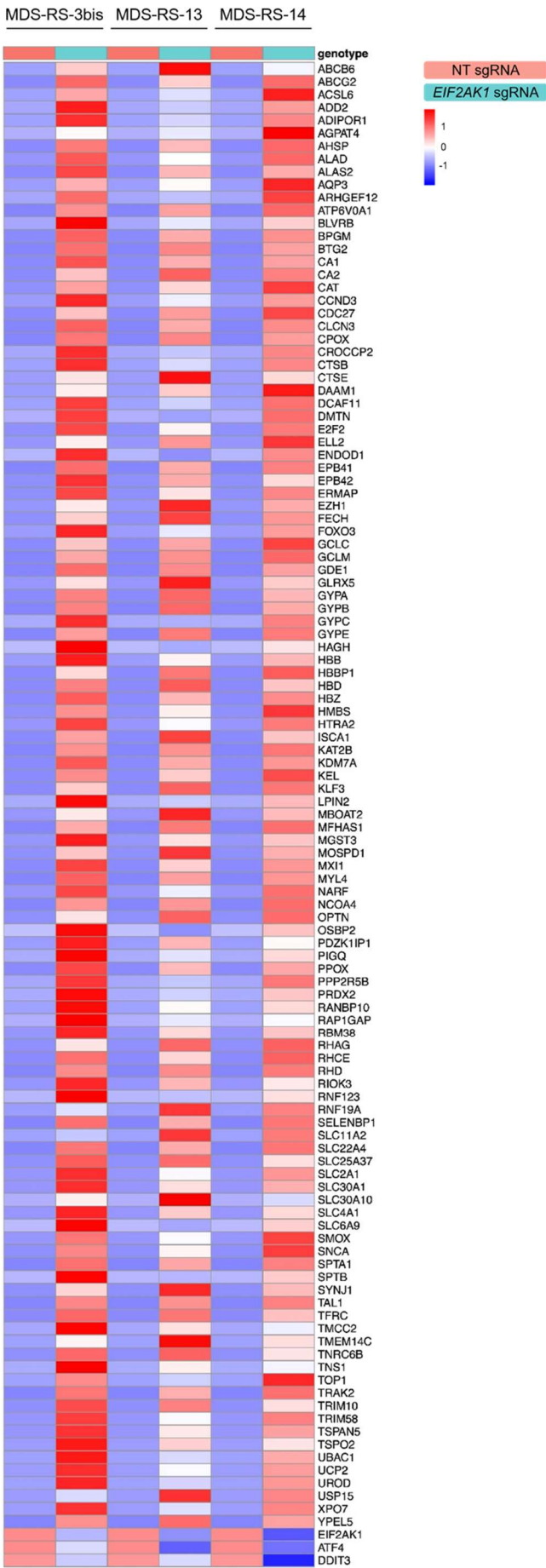
Supplementary Figure S3. Hypomethylating agent therapy inhibits the EIF2AK1-induced response pathway to heme deficiency in terminally differentiated cells in patients who became transfusion independent.

(A) Heatmap of the expression of the top 5 genes enriched in each of the 9 clusters shown in Figure 3A. HSC, hematopoietic stem cells; MPP, multipotent progenitors; Lympho, lymphoid; Ery/Mk, erythroid/megakaryocytic; Mk, megakaryocytic; Myelo, myeloid; Prog, progenitors. Arrows indicate the erythroid/megakaryocytic progenitors. **(B)** Distribution of Lin⁻CD34⁺ cells isolated from MDS-RS patients at baseline (left) and at the time of response to HMA therapy (right) across the clusters shown in Figure 3A. **(C)** Variant allelic frequencies (VAFs) of somatic mutations in relevant leukemia driver genes and/or oncogenes detected in total BM MNCs from 3 *SF3B1*-mutant MDS-RS patients at baseline or at the time of hematological response to HMA therapy. **(D)** Heatmap of the expression of the top 3 genes enriched in each of the 16 clusters shown in Figure 3B. **(E)** Distribution of MNCs isolated from MDS-RS patients at diagnosis (left) and at the time of response to HMA therapy (right) across the clusters shown in Figure 3B. HSPC, hematopoietic stem and progenitor cells; Mono, monocyte cells; Ery, erythroblasts; B-Lympho, B lymphocytes; T-Lympho/NK, T lymphocytes and natural killer cells; PC, Plasma cells. Arrows indicate the erythroblast population. **(F)** Flow cytometry plots showing the expression of CD71 and CD235a in primary CD45⁻erythroblasts derived from *SF3B1*-mutant CD34⁺ MDS-RS cells cultured in erythroid differentiation media for 8 days and then treated with vehicle (left) or 5-azacitidine (right) for 3 days. **(G)** Dot plot of the expression of the genes belonging to the EIF2AK1-mediated pathway that were significantly downregulated in MDS-RS Ortho-E at the time of response to HMA therapy as compared with the time of diagnosis. **(H)** Dot plot of the expression of autophagy pathway genes that were significantly downregulated in MDS-RS Ortho-E at the time of response to HMA therapy as compared with the time of diagnosis.

Supplementary Figure S4



J



K

Sample ID	Gene	VAF %	
		NT	EIF2AK1
MDS-RS-3-bis	<i>SF3B1</i>	14	12
MDS-RS-13	<i>SF3B1</i>	16	15
MDS-RS-14	<i>SF3B1</i>	36	42

Supplementary Figure S4. Inhibition of EIF2AK1 overcomes the accumulation of RS and enables terminal erythroid maturation and red blood cell production

(A) Flow cytometry plots showing the expression of CD71 and CD235a in representative NT (left) and *EIF2AK1* (right) sgRNA-treated *SF3B1*-mutant MDS-RS samples at day 13 of culture. **(B)** Representative Western blot analysis of EIF2AK1, phospho-EIF2S1 and LC3B in NT sgRNA- and *EIF2AK1* sgRNA-treated HD cells at day 13 of erythroid differentiation. Vinculin was used as a loading control. **(C)** Frequencies of CD71⁺CD235a⁻ (left), CD71⁺CD235a⁺ (middle), and CD71⁻CD235a⁺ (right) erythroblasts in NT sgRNA- or *EIF2AK1* sgRNA-treated HD samples (n=3) at day 13 of culture. Each symbol represents one sample; lines connect paired samples. No significant differences were detected using paired t-tests. **(D)** UMAP showing the CytoTRACE values of the cells in Figure 4C. The color indicates the degree of differentiation from low (grey) to high (red). **(E)** Violin plots of CD71 (top) and CD235a (bottom) expression across the 11 clusters shown in Figure 4C. **(F)** Pathway enrichment analysis of the marker genes of cluster 1 (top) and 7 (bottom) shown in Figure 4C (adjusted $P \leq 0.05$). **(G)** Dot plots of the expression of the genes involved in the EIF2AK1 response to heme deficiency pathway that were significantly downregulated in *EIF2AK1* sgRNA-treated cells from *SF3B1*-mutant MDS-RS in clusters 1 (left) and 7 (right) shown in Figure 4C. **(H)** Dot plots of the expression of the heme metabolism pathway genes that were significantly upregulated in *EIF2AK1* sgRNA-treated *SF3B1*-mutant MDS-RS cells from clusters 1 (left) and 7 (right) shown in Figure 4C. **(I)** Pathway enrichment analysis of the genes that were significantly upregulated (top) or downregulated (bottom) in *SF3B1*-mutant MDS-RS cells treated with *EIF2AK1* sgRNA as compared with those treated with NT sgRNAs ($P \leq 0.05$). **(J)** Heatmap of genes involved in heme metabolism that were significantly upregulated in *SF3B1*-mutant MDS-RS cells after *EIF2AK1* depletion. Expression of *EIF2AK1*, *ATF4*, and *DDIT3* indicate *EIF2AK1* pathway inhibition. **(K)** Variant allelic frequencies (VAFs) of *SF3B1^{MT}* detected in non-targeting (NT) sgRNA- and *EIF2AK1* sgRNA-treated MDS-RS cells at day 13 of culture.